J. Phys.: Condens. Matter **8** (1996) 10185–10194. Printed in the UK

X-ray analysis of epitaxial $PbTiO_3$ thin film grown on an (001) $SrTiO_3$ substrate by metal–organic chemical vapour deposition

Li Sun†, Yan-Feng Chen†‡, Peng Li†, Tao Yu†, Jian-Xie Chen† and Nai-Ben Ming†§

† National Laboratory of Solid State Microstructures, Nanjing University, Nanjing 210093, People's Republic of China

‡ Department of Materials Science and Technology, Nanjing University, Nanjing 210093, People's Republic of China

§ CCAST (World Laboratory), PO Box 8730, Beijing 100080, People's Republic of China

Received 25 March 1996, in final form 7 June 1996

Abstract. Using metal–organic chemical vapour deposition (MOCVD) under reduced pressure at 650 °C, stoichiometric $PbTiO_3$ thin films have been epitaxially grown on (001) $SrTiO_3$ single-crystal substrates. A series of x-ray analyses have been carried out to study the microstructures and phase transition process in the as-grown films. X-ray θ–2θ diffraction patterns revealed a pure perovskite phase of the thin film. The epitaxial nature of the film was confirmed by a Laue back-reflection photograph and x-ray Φ scan. From the rocking curve measurement made by the synchrotron radiation method at the Beijing Synchrotron Radiation Facility (BSRF), an *a*-, *c*-domain coexisting structure in the 4500 Å $PbTiO_3$ thin film had been observed with the *c*-axis of the *c*-domain perpendicular to the film surface and the *a*-axis *a*-domain tilted away from the surface normal. The phase transition process of the $PbTiO_3$ thin film was investigated through the high-temperature θ–2θ scan patterns; a higher T_c than in the $PbTiO_3$ single crystal had been observed. The strain-driven domain boundary movement in the film was studied by the relative diffraction intensity variation of the (200) and (002) planes.

1. Introduction

Because of the technological applications and theoretical value, extensive attention has been focused on the preparation and characterization of high-quality ferroelectric thin films. $PbTiO_3$, with a high Curie temperature of 490 °C and a very small aging rate of the dielectric constant [1], is a promising material as regards device usage. However, pure and dense $PbTiO_3$ ceramics are hard to obtain due to the great tensile stress occurring in the cooling process when the phase transition occurs and the fact that the bulk material may break into powder. Fortunately, the rapid progress in thin-film preparation techniques makes it possible to obtain epitaxial $PbTiO_3$ thin films by rf magnetron sputtering [2, 3], ion-beam sputtering [4], electron-beam evaporation [5], sol–gel [6, 7], pulsed-laser deposition (PLD) [8, 9], metal–organic decomposition (MOD) [10] and metal–organic chemical vapour deposition (MOCVD) [11–15] on various substrates. Also, the recently observed layer-by-layer growth mechanism [16] has demonstrated the MOCVD technique to be an ideal method for the growth of high-quality $PbTiO_3$ thin films.

Among the various insulating substrates used for the deposition of perovskite ferroelectrics, strontium titanate, $SrTiO_3$, is distinguished as being a perovskite-type

0953-8984/96/4910185+10$19.50

ferroelectric with a Curie temperature of 110 K and a cubic structure ($a = 3.905$ Å) from room temperature to the film deposition temperature. A similar structure and almost zero lattice mismatch with the *a*- and *b*-axis lattice constants (3.904 Å) of $PbTiO_3$ favour epitaxial growth of the *c*-axis-oriented $PbTiO_3$ thin films.

In this paper, we report the preparation and x-ray investigations of epitaxial $PbTiO_3$ thin films deposited on (001) $SrTiO_3$ substrates. In the *a*-, *c*-domain-coexisting $PbTiO_3$ thin film, a *c*-axis contraction phenomenon which was attributable to the size effect and the epitaxy-driven deformation had been observed. The high-temperature x-ray diffraction measurements revealed a higher phase transition temperature (T_c), indicated the influence of strain on T_c, and provided interesting information on the ferroelectric domain boundary movement when the film suffers a compressive strain during the heating cycle.

Table 1. Typical growth conditions.

Substrate	(001) $SrTiO_3$
Substrate temperature	∼650 °C
Total pressure	12.0 Torr
Carrier gas	N_2
T_{TIP}	65 °C
T_{TEL}	35 °C
TEL carrier flow rate	∼100 sccm
TIP carrier flow rate	∼50 sccm
O_2 flow rate	∼100 sccm

2. Experiment

$PbTiO_3$ thin films were deposited in a horizontal cool-wall MOCVD apparatus [17] under reduced pressure using purified titanium iso-propoxide (TIP) and tetra-ethyl lead (TEL) as the metal–organic precursors; N_2 and O_2 were used as the carrier gas and oxidant, respectively. The $SrTiO_3$ single-crystal wafers of size $10 \times 5 \times 1$ mm^3 were mechanically polished and cleaned by the standard semiconductor procedure. The cleaned substrates were put on a resistor-heating stainless-steel susceptor with a thermocouple inserted into the centre of the heating block for temperature measurement. By adjusting the vapour pressure of the MO precursors, the substrate temperature, the total reaction pressure, the partial pressure of O_2, and the flow rate of the MO vapour and N_2, optimal growth conditions were experimentally determined and these are listed in table 1.

The as-deposited $PbTiO_3$ thin films were transparent and had a pale-yellow glassy surface. The film thickness was measured by profilometry at the film edge made by selective deposition through a cover-glass mask and confirmed by scanning electron microscopy (SEM) cross-section morphology. The typical $PbTiO_3$ thin film had a thickness of 4500 Å, and the growth rate was determined to be 75 Å min^{-1}.

3. X-ray analyses

XRD measurements were performed on a Rigaku D/MAX-RA powder diffractometer with nickel-filtered Cu Kα radiation. As shown in figure 1, only the (00*k*) reflections of $PbTiO_3$ and $SrTiO_3$ appeared; no PbO and $Pb_2Ti_2O_7$ phases could be observed even on a logarithmic scale. Using the lattice constant of the $SrTiO_3$ substrate for a calibration, the *c*-axis length

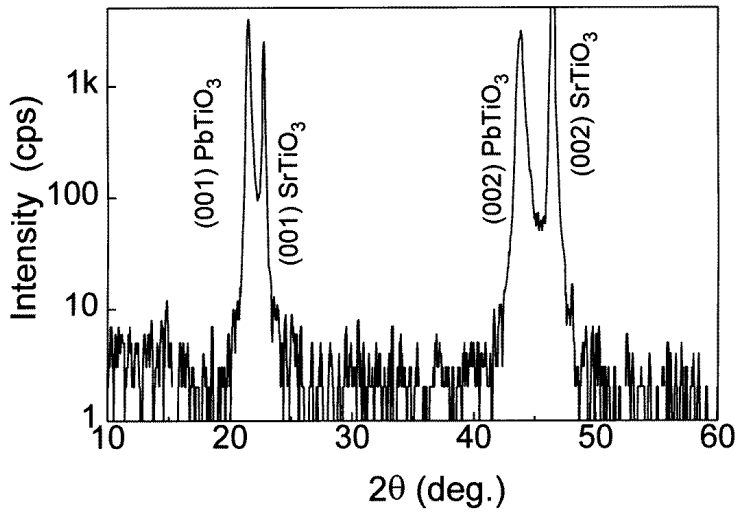

Figure 1. The XRD θ–2θ scan pattern of $PbTiO_3$ thin films deposited on an (001) $SrTiO_3$ substrate.

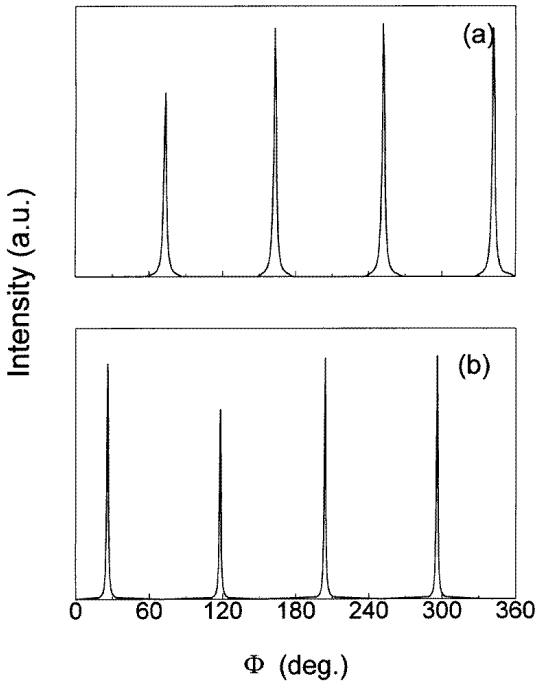

Figure 2. The x-ray intensity versus the angle Φ of (a) the (113) peak of the $PbTiO_3$ thin film, and (b) the (103) peak of the substrate.

of the as-grown thin film was determined to be 4.125 ± 0.002 Å, which was considerably smaller than that of the bulk material (4.150 Å). The chemical composition of the film

investigated by a Joel JXA-8800M electron microprobe revealed that the Pb, Ti and O distributed uniformly on the surface, and that the average atomic ratio of the Pb and Ti was 1:1.02, in accordance with the result calculated from the Rutherford back-scattering (RBS) [16] spectrum. So in our case, the *c*-parameter change should not be caused by lead deficiency as observed by Shirasaki. We noticed that the same phenomenon of *c*-axis contraction had been observed for $PbTiO_3$ thin film deposited on almost any substrate [19–22], so we assumed that in addition to the in-plane strain influence effected through the Poisson ratio, the size effect and the relaxation of the surface layer, the nature of the epitaxy would deform the film unit cell; in other words, in the epitaxy process, the film unit cells tended to have the same lattice parameters as the substrates, so the interface energy could be reduced, and this would not only be the origin of the in-plane strain, but also resulted in *c*-axis contraction when $c_{PbTiO_3} > a_{SrTiO_3}$.

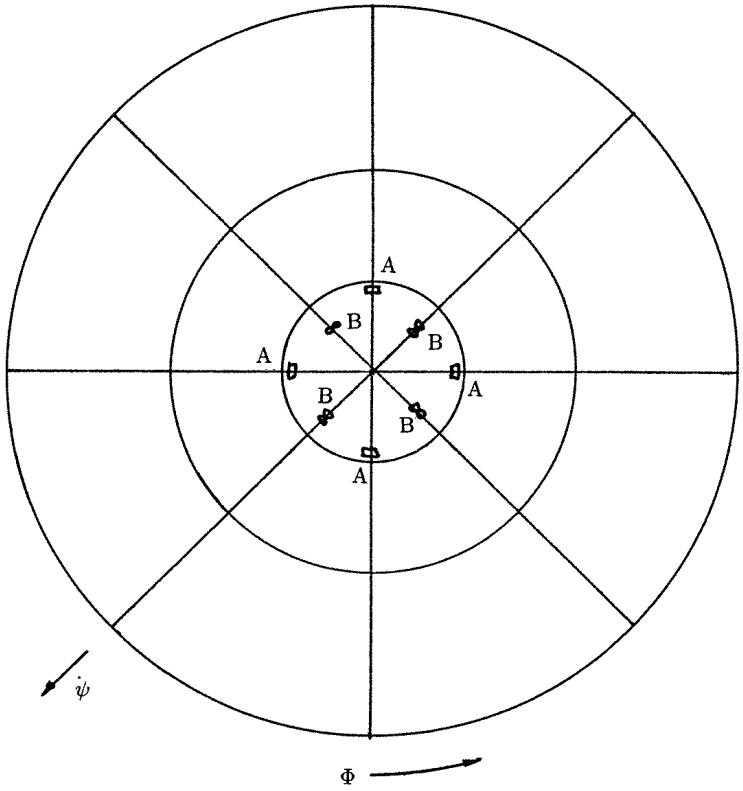

Figure 3. A simplified pole figure of a $PbTiO_3$ film on a $SrTiO_3$ substrate with a fixed 2θ-value of 77.4°. The intensities indicated as A and B are (113) reflections of the film and (103) reflections of the substrate, respectively. Two kinds of peak appear at the correct position as is expected in Wulff's projection for a $PbTiO_3$ film with the *a*-axis aligned with the [100] and [010] directions of the substrate.

Because the XRD θ–2θ scan can only detect the crystal surfaces with normals parallel to the growth direction, back-reflection x-ray Laue photography and an x-ray Φ scan were performed to determine the epitaxial relationship between the $PbTiO_3$ thin film and the $SrTiO_3$ substrate. In the Laue photograph, only a fourfold-symmetric diffraction pattern

was clearly discerned without rings being observed. This suggests that the as-deposited thin film was not textured, but epitaxial. Precise information about the in-plane lattice vector alignment of the film and the substrate was obtained by x-ray Φ scanning. The measurement was made by rotating the sample around the surface normal at a fixed 2θ-value of 77.4°; the 2θ-angle corresponded to the reflections of the (113) plane of the $PbTiO_3$ films and the (103) plane of the $SrTiO_3$ substrates; the tilt angles ψ of the two planes were 63.5° and 71.6° off the original surface normal, respectively. In the two Φ-scan patterns (figure 2), both curves exhibit four sharp peaks separated one from the other by a 90° rotating angle, and the measured Φ angles for the two reflections are 72° and 27° with a 45° difference. The Φ value indicates the relative positions of the surface normal projection in the (001) plane. The angle between the projections of the {103} surface normal of the $PbTiO_3$ and the {113} surface normal of the $SrTiO_3$ in the {001} plane is 45° when lattices of $PbTiO_3$ and $SrTiO_3$ are coherent, so the experimentally obtained Φ value confirms that the in-plane lattice vectors of the $PbTiO_3$ layer are epitaxially aligned with those of the $SrTiO_3$ substrate, i.e., (100) $PbTiO_3$ ∥ (100) $SrTiO_3$, (010) $PbTiO_3$ ∥ (010) $SrTiO_3$ and (001) $PbTiO_3$ ∥ (001) $SrTiO_3$. The corresponding polar figure is plotted schematically in figure 3; contributions of the (113) reflections of the $PbTiO_3$ film and the (103) reflections of the $SrTiO_3$ film are indicated. A fourfold symmetry has been observed, as is anticipated for a tetragonal lattice of $PbTiO_3$ and the cubic structure of $SrTiO_3$. In this picture, all of the reflections are at the expected positions, and it also confirms the in-plane epitaxy of the film.

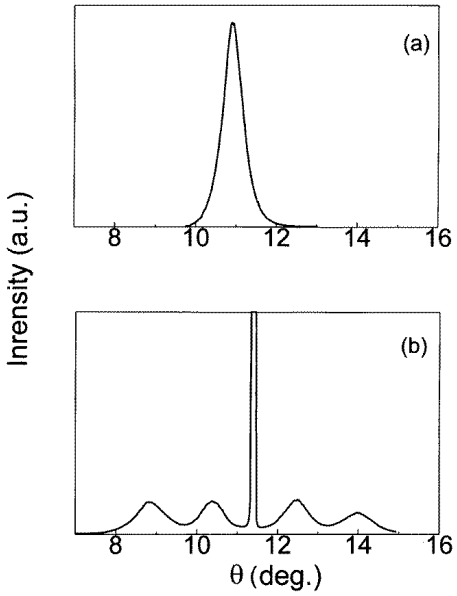

Figure 4. Rocking curves of the (a) (001) orientation of $PbTiO_3$ and (b) (100) orientation of $SrTiO_3$; the central peak was the reflection of the substrate, and the other four peaks correspond to the four tilted (100) orientations in the *a*-domain of $PbTiO_3$ thin film.

Because of the almost zero lattice mismatch between the *a*- and *b*-axes of the $PbTiO_3$ film and the lattice constant of the $SrTiO_3$ substrate at room temperature, the *a*-domain diffraction signal overlaps the substrate, and the domain configuration in the $PbTiO_3$ cannot be discerned by normal x-ray θ–2θ diffraction. Theoretical analysis points out that for *a*-, *c*-domains coexisting in $PbTiO_3$ film, the *c*-axis of the *c*-domain should be perpendicular

to the surface, so the elastic energy in the films can be reduced, and the slight difference between the lengths of the *a*- and *c*-axes may cause the *a*-orientation in the *a*-domain to have a tilt away from the surface normal [23–24]; this tilt can be discerned by the x-ray ω-scan method through different θ-values at a fixed value of 2θ. Our rocking curve experiment was performed at the Beijing Synchrotron Radiation Facility (BSRF) using a 1.54 Å monochromatic x-ray beam which was obtained by using the {220} plane of Si single crystal as a monochromator; the detector had an energy resolution of 4.4×10^{-4} eV. Figure 4 shows the rocking curves for (001) of $PbTiO_3$ and the (001) orientation of the $SrTiO_3$ substrate; only a sharp peak with a full width at half-maximum (FWHM) of 0.48° has been recorded in figure 4(a); this confirms that the *c*-axis in the *c*-domain is perpendicular to the surface. In figure 4(b), besides the diffraction peak of the (100) orientation of the $SrTiO_3$ substrate, four other peaks corresponding to the (100) diffraction of the $PbTiO_3$ with a tilt angle have been detected. Li *et al* [23] had proposed that the fourfold symmetry along the (001) direction of tetragonal $PbTiO_3$ would lead the *a*-domains to be aligned equivalently around a *c*-domain. Because of the different included angles with respect to the incident x-ray, differently oriented *a*-domains exhibit four θ-values.

The phase transition of the $PbTiO_3$ thin film was investigated using a high-temperature x-ray diffraction technique. During the experiment, the sample was placed in the centre of a triangular column coiled with Pt resistance thread in order to create a uniform temperature field. A thermocouple was fixed directly on the back of the sample for temperature measurement. The thermocouple was calibrated with a precision better than ± 1 °C. The rate of heating and cooling was kept at 4 °C min^{-1} and the temperature was held steady long enough to allow thermal equilibrium to be reached before the x-ray diffraction measurement was performed. Figure 5 shows the profile near the (002) peak of $PbTiO_3$. The (200) peak of $PbTiO_3$ which could not be observed at room temperature was separated from the (002) peak of the $SrTiO_3$ substrate due to the different thermal expansion coefficients of $PbTiO_3$ and $SrTiO_3$ when temperature rose up to 470 °C. A computer program was developed to distinguish the (200) and (002) signals; we firstly determined the functional from of a single reflection, then used a least-squares method to determine the positions and intensities of the two diffractions. Using this computer simulation, the phase transition from a tetragonal to a cubic structure was observed at about 515 °C and in the reverse process it happened at 507 °C. Figure 6 is the lattice parameter versus temperature plot; the *c*-axis lattice constant has a hysteresis in the cooling process unlike in the heating process, and the *a*-axis length in the *a*-domains changes in almost the same way in both cycles

Table 2. Lattice parameters of $PbTiO_3$ and $SrTiO_3$.

Materials	Room temperature (23 °C)	Growth temperature (650 °C)	Phase transition temperature (510 °C)
$PbTiO_3$	$a = b = 3.904$ Å	$a = b = c = 3.990$ Å	$a = b = 3.968$ Å
	$c = 4.152$ Å		$c = 3.996$ Å
$SrTiO_3$	$a = b = c = 3.905$ Å	$a = b = c = 3.930$ Å	$a = b = c = 3.924$ Å

From the high-temperature x-ray diffraction, it was also observed that the relative reflection intensities of the (002) and (200) planes of $PbTiO_3$ changed with the temperature, indicating the movement of domain walls. A *c*-domain reduction and *a*-domain enlargement in this process had been observed in the heating cycle, and a reversal process happened in the cooling cycle. According to powder diffraction patterns of $PbTiO_3$, the diffraction intensity ratio of the (200) plane and (002) plane is 8:15, so the *c*-domain ratio α can be

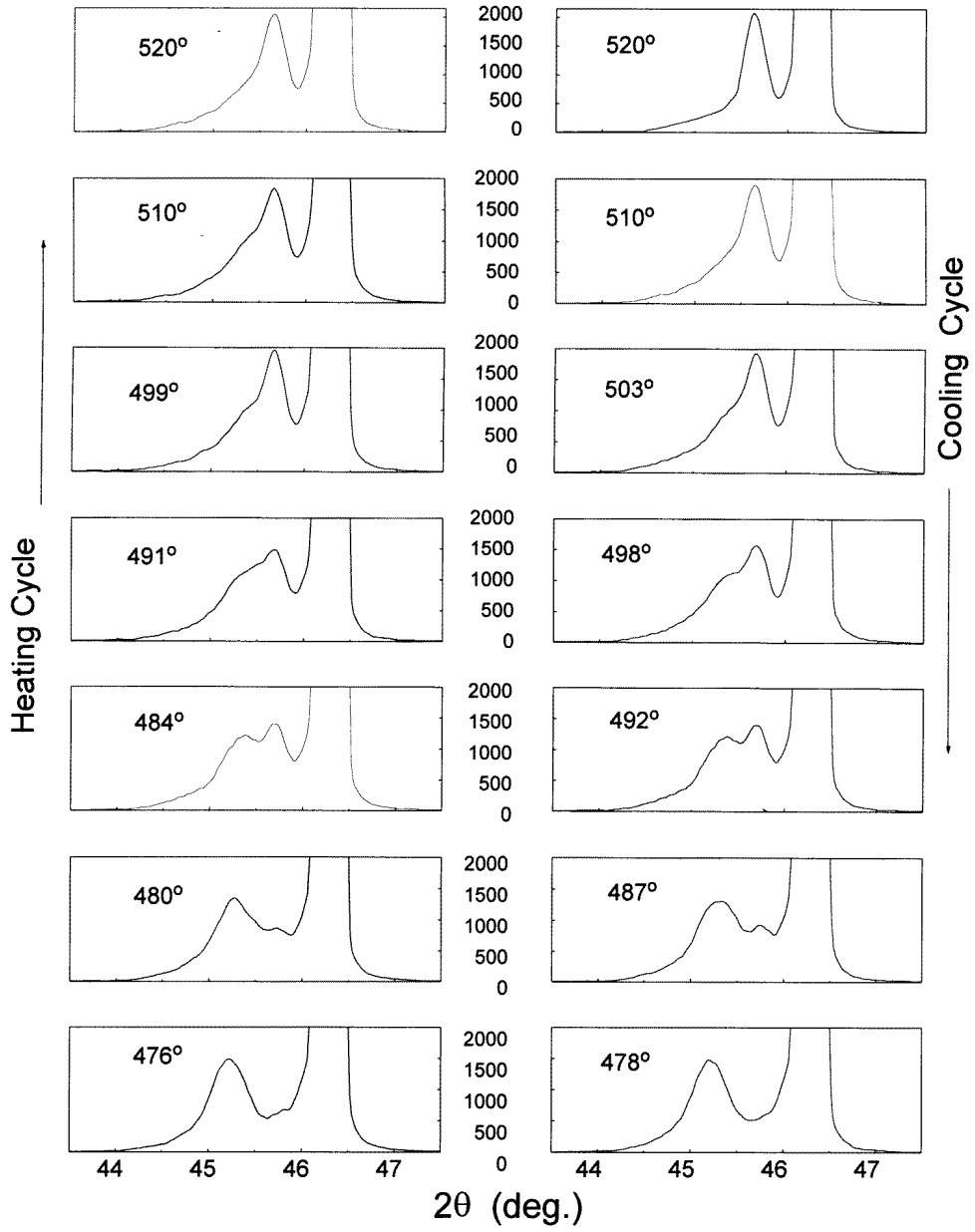

Figure 5. The temperature dependence of the x-ray diffraction profile near the (002) peak of PbTiO3 thin film.

defined as follows:

$$a = I(002)/\{I(002) + I(200) \times 8/15\}$$

where $I(200)$ and $I(002)$ represent the intensities of the (002) and (200) reflections respectively. The c-domain ratio versus temperature plot is shown in figure 7. The movement of the domain boundary can be attributed to the difference between the thermal

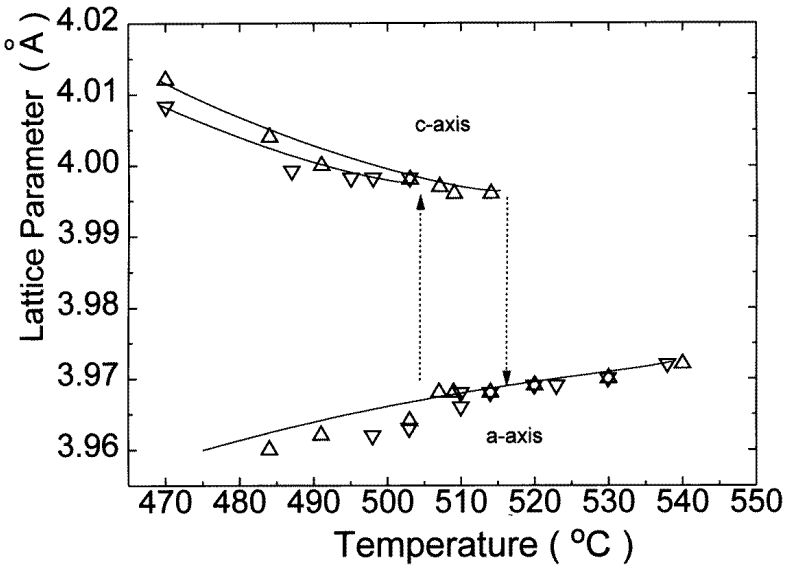

Figure 6. The temperature dependence of the lattice constants a and c of $PbTiO_3$ thin film. △: the heating cycle, ▽: the cooling cycle.

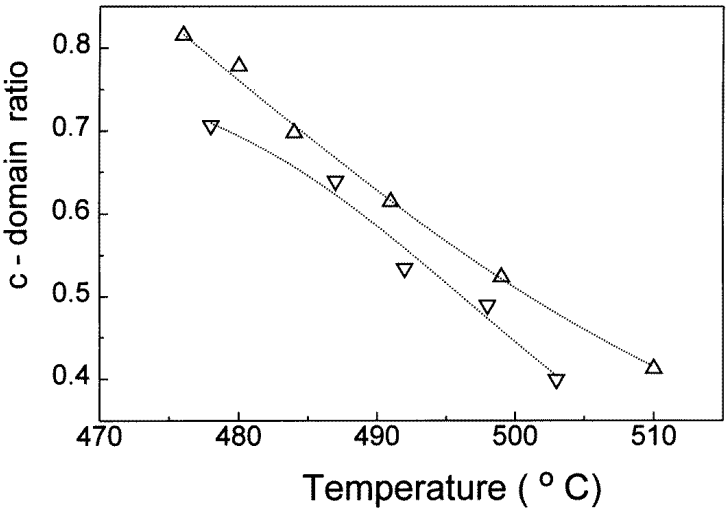

Figure 7. The temperature dependence of the c-domain ratio in the film. △: the heating cycle; ▽: the cooling cycle.

expansions of the $PbTiO_3$ and $SrTiO_3$ substrates. As listed in table 2, at the growth temperature of 650 °C, the $PbTiO_3$ has a cubic structure, and the lattice mismatch with $SrTiO_3$ is 1.53%. When the film is cooled to the phase transition temperature, the $PbTiO_3$ transforms to a tetragonal structure; the lattice mismatches between a-, b-$PbTiO_3$/$SrTiO_3$ and c-$PbTiO_3$/$SrTiO_3$ are 1.12% and 1.83%, but they change to -0.03% and 6.3% at room temperature, respectively. Recent studies have proved the domain formation to be the most

significant lattice-mismatch-relaxation mechanism in the thin-film epitaxy, so the different thermal expansion coefficients play the most important role in generating a strain in the film as Pompe *et al* reported [25]. During the heating cycle, the $SrTiO_3$ substrate may generate a compressive stress on the *c*-domain due to the smaller expansion coefficient compared to the *a*- and *c*-axis expansion coefficients of $PbTiO_3$. As a result, the $PbTiO_3$ film prefers an *a*-axis orientation, so the *a*-domain ratio increases. We notice that the *c*-axis deformation caused by surface relaxation and the difference between the film–substrate unit cells decreases when the temperature rises. So the upshift of the $PbTiO_3$ phase transition temperature can also be understood from considering this compressive stress in the thin film.

4. Summary

The results of the investigation can be summarized as follows.

(1) Stoichiometric $PbTiO_3$ thin films have been epitaxially deposited on (001) $SrTiO_3$ substrates using a low-pressure MOCVD technique at a growth temperature of 650 °C.

(2) A *c*-axis shortening phenomenon has been found in the thin film and is attributable to the size-induced surface relaxation and the nature of the heteroepitaxy.

(3) Synchrotron radiation rocking curves reveal that *a*- and *c*-domains coexist in the as-grown 4500 Å $PbTiO_3$ thin films; (001) of the *c*-domain is perpendicular to the film surface and the tilted *a*-domain aligns around the *c*-domain with a fourfold symmetry.

(4) The phase transition temperature of the $PbTiO_3$ thin film showed an upward shift compared with that of the bulk $PbTiO_3$ single crystal. The content of *a*-, *c*-domains in the film changed with the temperature due to the stress caused by the difference between the thermal expansion coefficients of the $PbTiO_3$ and $SrTiO_3$.

Acknowledgments

The authors would like to thank X M Jiang and L S Xiu for making the rocking curve measurements at BSRF. The help of Y P Zhu, Y D Ye and L J Shi is highly appreciated. The work was supported partly by the National 863 High Technology Programme of the People's Republic of China.

References

[1] Ikegami S and Ueda I 1967 *J. Phys. Soc. Japan* **22** 725
[2] Iijima K, Tomita Y, Takeyama R and Ueda I 1986 *J. Appl. Phys.* **60** 361
[3] Okawamura M, Matsui Y, Nakano H, Nakagawa T and Hamakawa Y 1979 *Japan. J. Appl. Phys.* **18** 1633
[4] Castellano R N and Feinstein L G 1979 *J. Appl. Phys.* **50** 4406
[5] Shiosaki T, Adachi M, Modhizuki S and Kawabata A 1985 *Ferroelectrics* **63** 227
[6] Maeda M, Ishida H, Soe K K and Suzuki I 1993 *Japan. J. Appl. Phys.* **32** 4136
[7] Hayashi Y and Blum B 1987 *J. Mater. Sci.* **22** 2655
[8] Ghonge S G, Goo E and Ramash R 1993 *Appl. Phys. Lett.* **62** 1742
[9] Okuyama M, Asano J, Imai T, Lee D H and Hamakawa Y 1993 *Japan. J. Appl. Phys.* **32** 4107
[10] Okada M, Takai S, Amemiya M and Tominaga K 1989 *Japan. Appl. Phys. Lett.* **28** 1030
[11] Kwak S B, Embil A, Budai J D, Chisholm M F, Boatner L A and Wilkens B J 1994 *Phys. Rev.* B **49** 14 865
[12] de Keijser M, Domans G J, Cillessen J F M, de Leeuw D M and Zandbergen H W 1991 *Appl. Phys. Lett.* **58** 2636
[13] Bai G R, Chang H L M, Foster C M, Shen Z and Lan D J 1994 *J. Mater. Res.* **9** 156
[14] Lee W G, Woo A I, Kim J C, Choi S H and Oh K H 1993 *Appl. Phys. Lett.* **63** 2511

[15] Sun L, Chen Y F, Yu T, Chen J X and Ming N B 1995 *J. Phys. D: Appl. Phys.* **7** 6537
[16] Chen Y F, Sun L, Yu T, Chen J X, Ming N B, Ding D S and Wang L W 1995 *Appl. Phys. Lett.* **67** 3503
[17] Chen Y F, Chen J X, Sun L, Yu T, Li P, Ming N B and Shi L J 1995 *J. Cryst. Growth* **146** 624
[18] Shirasaki S 1971 *Solid State Commun.* **9** 1217
[19] Gao Y, Bai G, Merkle K L, Chang H L M and Lam D J 1993 *Thin Solid Films* **235** 86
[20] Erbil A, Braun W, Kawk B S, Wilkens B J, Boatner L A and Budai J D 1992 *J. Cryst. Growth* **124** 684
[21] Chen Y F, Yu T, Chen J X, Shun L, Li P and Ming N B 1995 *Appl. Phys. Lett.* **66** 148
[22] Zhong W L, Wang Y G, Kong D S, Zhang P L and Qu B D 1994 *Thin Solid Films* **237** 160
[23] Li Z, Foster C M, Guo D, Zhang H, Bai G R, Baldo P M and Rehn L E 1994 *Appl. Phys. Lett.* **65** 1106
[24] Bai G R, Chang H L M, Foster C M, Shen Z and Lam D J 1994 *J. Mater. Res.* **9** 156
[25] Pompe W, Gong X, Suo Z and Speck J S 1995 *J. Appl. Phys.* **74** 6012